Network structure of molybdate glasses by neutron and X-ray diffraction and reverse Monte Carlo modelling

M Fabian[1,2], E Svab[2], K Krezhov[3]

E-mail: fabian.margit@energia.mta.hu

[1]Centre for Energy Research, 1121 Budapest, Konkoly-Thege st. 29-33, Hungary
[2]Wigner Research Centre for Physics, 1121 Budapest, Konkoly-Thege st. 29-33, Hungary
[3]Institute for Nuclear Research and Nuclear Energy, 1784 Sofia, 72 Tzarigradsko Chaussee, Bulgaria

Abstract. Rare-earth molybdate glasses have been prepared by rapid quench technique, the network structure was investigated by neutron and high-energy X-ray diffraction. For data evaluation the reverse Monte Carlo simulation technique was applied to obtain a possible 3-dimensional network configuration, which is consistent with the experimental data. From the modelling the partial atomic correlation functions $g_{ij}(r)$ and the coordination number distributions CN_{ij} have been revealed. Formation of MoO_4 (55%) and MoO_6 (25%) units was established for the binary $90MoO_3$-$10Nd_2O_3$ glass. The B-O first neighbour distribution show a relatively broad first neighbour distance at 1.40Å, the average coordination numbers show the presents of trigonal BO_3 and tetrahedral BO_4 groups. For $50MoO_3$-$25Nd_2O_3$-$25B_2O_3$ sample mixed MoO_4-BO_4 and MoO_4-BO_3 linkages form pronounced intermediate-range order.

1. Introduction

Rare-earth molybdate phases are known to exhibit a great variety of important physical properties including high ion and electron conductivity of fast oxide ion conductors derived from the parent oxide $La_2Mo_2O_9$ (LAMOX family [1,2], non-linear optical response and luminescent properties ($Sm_2(MoO_4)_3$, $LiLn(MoO_4)_2$, Ln=Nd, Pr, Ho), e.g. [3].

In contrast to the most molybdates with relatively well-characterised crystalline and magnetic structures, e.g. [4-7], the preparation and structural information on amorphous molybdate systems is not ample. MoO_3 is well known as a conditional network former and it is not able to form a glass itself at even rapid cooling rates. The main problems of the preparation of molybdate glasses without modifier ions or participation of classical network formers are connected with the high crystallization tendency of the components.

Recently, the group of Dimitriev [8-10] has undertaken a systematic study to clear up the tendency for glass formation and immiscibility in the molybdate systems containing rare-earth oxides and in the complex mixed boromolybdate glasses. The phase diagram for several ternary oxides, MoO_3-$Nd(La)_2O_3$-B_2O_3 was set up [9] and the basic structural and optical characteristics were investigated by XRD, DTA, SEM, UV-VS spectra and IR spectroscopy [10].

The aim of this work is to get a deeper insight into the structural network characteristics of new series of molybdate conditional glass former containing modifiers Nd_2O_3, MgO and classical glass former B_2O_3. The Nd_2O_3 is appropriate component due to its specific optical properties but it increases the melting temperature. The MgO influences significantly properties as viscosity, glass transition temperature and chemical durability. By introducing of B_2O_3 it is possible to obtain low melting materials.

For this study four new amorphous samples of the glassy MoO_3-Nd_2O_3-(MgO)/(B_2O_3) system have been prepared by rapid quench technique. Both neutron and high-energy X-ray diffraction experiments have been performed, and for structure modelling the reverse Monte Carlo (RMC) computer simulation technique [11] was applied. We expect to obtain new structural data, especially on the characteristics of the partial atomic pair correlation functions, the first neighbour atomic distances, coordination numbers and network former units and their linkages.

2. Experimental details and methods

2.1. Samples

The amorphous materials have been prepared by a conventional melt quenching method. The nominal composition of the glasses synthesized in the present study are binary $90MoO_3$-$10Nd_2O_3$ (hereafter referred to as Mo90Nd10), ternary $80MoO_3$-$15Nd_2O_3$-5MgO (Mo80Nd15Mg5), $75MoO_3$-$12.5Nd_2O_3$-12.5MgO (Mo75Nd12.5Mg12.5) and $50MoO_3$-$25Nd_2O_3$-$25B_2O_3$ (Mo50Nd25B25) (mol%). Commercial powder of reagent grade MoO_3, Nd_2O_3 and MgO were used as starting materials and were mixed in an alumina mortar. The boron containing sample was prepared from boron oxide, ^{11}B-isotope enriched to 99.6%, to avoid the high neutron absorption of natural boron. The batches were melted at 1200-1300^{o}C for 30 min in air in a platinum crucible. The melting temperature was limited to 1300^{o}C taking into account the volatility of the components. The glasses were obtained by pouring the melts onto an iron plate and by pressing with another iron plate (cooling rate: 10^2 K/s).

2.2. Neutron and X-ray diffraction experiments

Neutron diffraction (ND) measurements have been performed in a relatively broad momentum transfer range, Q=0.4-35Å^{-1}, combining the data measured by the two-axis 'PSD' diffractometer (λ_0=1.068Å) [12] at the 10 MW Budapest research reactor for all samples and by the time-of-flight 'HIPD' instrument [13] at the LANSCE pulsed neutron source for Mo80Nd15Mg5 and Mo75Nd12.5Mg12.5 samples and by the '7C2' diffractometer at the LLB-CEA-Saclay (λ_0=0.726 Å) [14] for Mo90Nd10 and Mo50Nd25B25 samples. The powder specimens of about 3–4 g/each were filled in a cylindrical vanadium sample holder of 8 mm (PSD, 7C2) and 10 mm (HIPD) diameter for the three types of experiments. The structure factors, $S(Q)$s, were evaluated from the raw experimental data independently for the three types of measurements, using the programme packages available at the facilities. The three sets of $S(Q)$s were obtained in the Q=0.4-9.6Å^{-1} (PSD), Q=0.2-15.3Å^{-1} (7C2) and in the 1.5-35Å^{-1} interval using the HIPD experiments. The agreement between the corresponding $S(Q)$ data was within 1% in the overlapping Q range. The statistics of the PSD data is excellent at relatively low Q values, while the statistics and the information content of the 7C2 and HIPD data is unique above 8Å^{-1}. Therefore the $S(Q)$ patterns were combined by normalizing the PSD data to the 7C2 and HIPD data sets in the 4–8Å^{-1} interval by the least-squares method, and the average values of the two spectra were used for further data treatment, while for Q<4Å^{-1} the PSD data and for Q>8Å^{-1} the 7C2 and HIPD data were used. The neutron $S(Q)$ data were obtained with a good signal-to-noise ratio up to Q_{max}=15.3Å^{-1} for Mo90Nd10 and Mo50Nd25B25 and Q_{max}=35Å^{-1} for Mo80Nd15Mg5 and Mo75Nd12.5Mg12.5 samples.

The high-energy X-ray diffraction (XRD) measurements were carried out at the BW5 experimental station [15] at HASYLAB, DESY. The powdered samples were filled into quartz capillary of 2 mm in diameter (wall thickness of ~0.02 mm). The energy of the radiation was 109.5 keV (λ_0=0.113Å). Raw data were corrected for detector dead time, background, absorption, and variations in detector solid angle. The X-ray $S(Q)$ data were obtained with a good signal-to-noise ratio up to Q_{max}=25Å^{-1} .

The overall run of the curves for the two radiations is fairly different, because of the differences in the weighting factors, w_{ij} of the partial structure factors, $S_{ij}(Q)$:

$$S(Q) = \sum_{i,j}^{k} w_{ij} S_{ij}(Q), \qquad (1)$$

$$w_{ij}^{ND} = \frac{c_i c_j b_i b_j}{\left[\sum_{i,j}^{k} c_i b_j\right]^2}, \quad (2)$$

$$w_{ij}^{XD}(Q) = \frac{c_i c_j f_i(Q) f_j(Q)}{\left[\sum_{i,j}^{k} c_i f_j(Q)\right]^2}, \quad (3)$$

where c_i, c_j are the molar fractions of the components, b_i, b_j the coherent neutron and $f_i(Q)$, $f_j(Q)$ the X-ray scattering amplitudes, and k is the number of elements in the sample. Note, that the neutron scattering amplitude is constant [16], while the X-ray scattering amplitude is Q-dependent [17]. In order to compare the corresponding weighting factors for the two radiations, Table 1 includes the Q-independent w_{ij}^{ND} together with a characteristic value for $w_{ij}^{XD}(Q)$ at Q=1.06Å^{-1}. It can be seen that the Mo-O and Nd-O atom pairs have a significant contribution for both radiations, while B-O plays a significant contribution only in the neutron experiment. The O-O contribution has a dominant weight in the neutron experiment, in contrast to the X-ray case, where it is much weaker.

Table 1. Neutron and X-ray (at Q=1.06 Å^{-1}) weighting factors, w_{ij}(%) for the investigated glasses.

Composition	**90%MoO_3-10%Nd_2O_3**		**75%MoO_3-12.5%Nd_2O_3-12.5%MgO**		**50%MoO_3-25%Nd_2O_3-25%B_2O_3**	
Atom pairs	**Neutron**	**X-ray**	**Neutron**	**X-ray**	**Neutron**	**X-ray**
Mo-O	33.79	33.20	28.96	28.24	14.97	16.83
Nd-O	8.44	10.51	10.95	13.45	17.15	24.02
Mg-O	-	-	3.82	1.22	-	-
B-O	-	-	-	-	14.82	1.82
O-O	48.58	10.41	45.81	9.78	38.87	9.35
Mo-Mo	5.87	26.46	4.57	20.38	1.44	7.43
Mo-Nd	2.93	16.75	3.46	19.42	3.30	21.20
Mo-B	-	-	-	-	2.85	1.61
Nd-Nd	0.36	2.65	0.65	4.62	1.89	15.13

On the other hand, the contribution of the metal-metal second neighbour Mo-Mo, Mo-Nd and Nd-Nd atomic correlations appears with a significant weight only in the X-ray experiment.
As a first step of data evaluation the total reduced correlation function, $G(r)$ was calculated by the usual Fourier transformation (see our previous papers [18,19]). The neutron $G(r)$s are shown in Fig. 1.

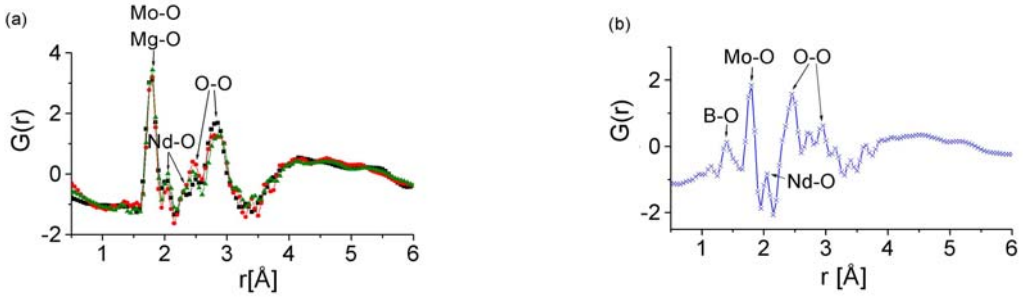

Figure 1. Experimental neutron total reduced distribution function, $G(r)$: a) Mo90Nd10 (square), Mo80Nd15Mg5 (circle), Mo75Nd12.5Mg12.5 (triangle) and b) Mo50Nd25B25 (cross) glasses obtained by Fourier transformation from the corresponding $S(Q)$.

The $G(r)$ curves show up a sharp peak at 1.8Å for all specimens, which can be attributed to the Mo-O distance. The Mg-O is expected between 1.7-1.9Å, which overlaps with the Mo-O distribution. As far as the first peak is rather sharp, we can conclude that Mg-O first neighbour distance is also at ~1.8Å. The next small intensity but sharp peak appears at ~2.05Å, which may be attributed to the Nd-O first neighbour distance. The O-O distances appear in the 2.5-3Å interval, however, an overlap might be with other second neighbour distributions. In the case of the B-containing specimen, an additional peak appears in $G(r)$ at ~1.4Å (Fig. 1/b), which can be related to the B-O first neighbour distance. In order to get a deeper insight into the network structure, the RMC simulation technique has been used.

3. Reverse Monte Carlo modelling and results

The experimental $S(Q)$ data have been simulated by the RMC simulation technique. The RMC minimizes the squared difference between the experimental $S(Q)$ and the calculated one from a 3D atomic configuration. The RMC algorithm calculates the one-dimensional partial atomic pair correlation functions $g_{ij}(r)$, and they are inverse Fourier transformed to calculate the partial structure factors, $S_{ij}(Q)$. For the RMC starting model disordered atomic configuration was built up with a simulation box containing 10.000 atoms. The density values were 0.0733, 0.0668, 0.0670, 0.0664 atoms·Å^{-3} for Mo90Nd10, Mo80Nd15Mg5, Mo75Nd12.5Mg12.5, Mo50Nd25B25 samples, respectively, and the corresponding RMC half-box lengths were 25.739, 26.548, 26.522 and 26.601 Å.

In the RMC simulation procedure two types of constraints were used, the minimum interatomic distances between atom pairs (cut-off distances) and connectivity constraints. We have used connectivity constraints only for the network former B-O atom pairs. It is reasonable to suppose that boron atoms are surrounded both by three-coordinated and four-coordinated oxygen atoms, forming trigonal BO_3 and tetrahedral BO_4 units as reported for binary neodymium borate glasses [20], for ternary rare-earth boromolybdate MoO_3-Nd(La)$_2O_3$-B_2O_3 [9,10], for B_2O_3-Bi_2O_3-MoO_3 glass [21], similarly, as for binary alkali borate glasses [22 and references therein]. For the starting cut-off distances we have used the characteristic values obtained from the total $G(r)$s (see Fig.1), i.e. for B-O 1.28Å, Mo-O 1.65Å , Nd-O 2.0Å, O-O 2.32Å. Several RMC runs have been completed by modifying the cut-off distances in the way, that the results of each run have been carefully checked to obtain reliable data for each $g_{ij}(r)$ and coordination number distributions, $CN_{ij}(n)$. The convergence of the RMC calculations was good and the final $S(Q)$s matched very well the experimental ones. (see Fig. 2).

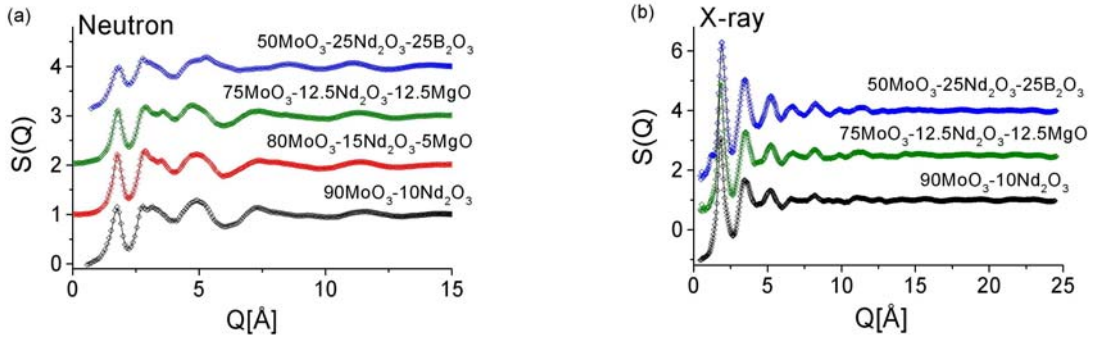

Figure 2. Experimental data (rhombus) and RMC simulation (solid line): a) Neutron and b) X-ray diffraction.

The partial atomic pair correlation functions, $g_{ij}(r)$ have been revealed from RMC simulation with a good reproducibility and acceptable statistics. The oxygen-linked $g_{i\text{-}O}(r)$ and coordination number distributions are shown in Figure 3 and Figure 4.

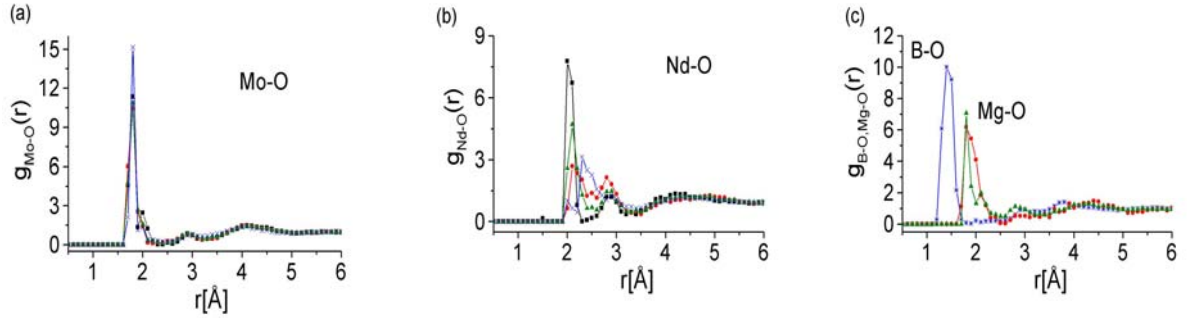

Figure 3. O-linked partial atomic pair correlation functions obtained from the RMC modelling for the: Mo90Nd10 (square), Mo80Nd15Mg5 (circle), Mo75Nd12.5Mg12.5 (triangle), Mo50Nd25B25 (cross).

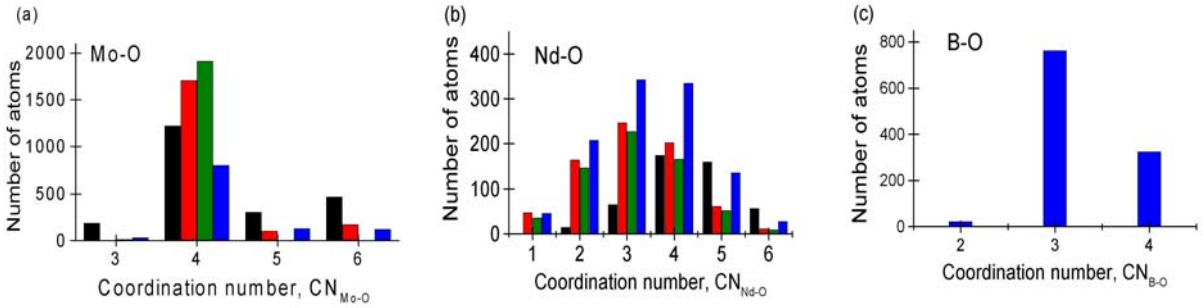

Figure 4. Coordination number distributions obtained from the RMC modelling for the glasses: Mo90Nd10 (black), Mo80Nd15Mg5 (red), Mo75Nd12.5Mg12.5 (green), Mo50Nd25B25 (blue).

The corresponding first neighbour distances are presented in Table 2 and the average $CN_{i\text{-}O}$ in Table 3.

Table 2. Oxygen-linked atomic distances, r_{ij} (Å)

Sample	r_{ij} (Å)				
	Mo-O (±0.02)	**Nd-O (±0.05)**	**B-O (±0.02)**	**Mg-O (±0.1)**	**O-O (±0.1)**
Mo90Nd10	1.80/2.0	2.0/2.8	-	-	2.3/2.8
Mo80Nd15Mg5	1.80	2.1/2.8	-	1.8	2.45/2.8
Mo75Nd12.5Mg12.5	1.80	2.1/2.9	-	1.8/2.1	2.4/2.8
Mo50Nd25B25	1.80/2.0	2.0/2.3/2.9	1.4	-	2.4/2.9

Table 3. Average partial coordination numbers, CN_{ij} (atom)

Sample	CN_{ii}				
	Mo-O (±0.2)	**B-O (±0.1)**	**Nd-O (±0.5)**	**Mg-O (±0.5)**	**O-O (±0.5)**
Mo90Nd10	4.9	-	4.3	-	8.0
Mo80Nd15Mg5	4.2	-	3.1	4.3	6.9
Mo75Nd12.5Mg12.5	4.0	-	3.1	3.8	6.2
Mo50Nd25B25	4.2	3.3	4.3	-	5.9

In the studied system the results obtained from RMC modelling have shown significant correlations between several second neighbour atom pairs, as it is shown in Figure 5. This is important, as far as the analysis of these results may give useful information on the linkage of the basic structural units forming the network structure. The second neighbour partial distributions are collected in Figure 5.

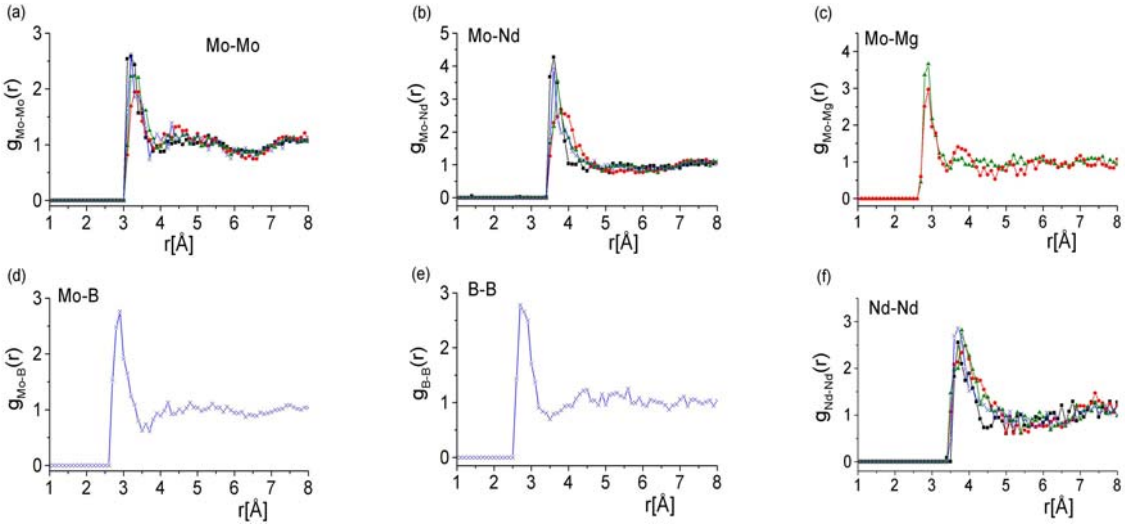

Figure 5. Second neighbour partial atomic pair correlation functions obtained from the RMC modelling for the molybdate glasses, for Mo90Nd10 (square), Mo80Nd15Mg5 (circle), Mo75Nd12.5Mg12.5 (triangle) and Mo50Nd25B25 (cross).

4. Discussion

In the present study for the Mo-O atom pair correlations a well-defined first neighbour distance is obtained at 1.80±0.02Å, and the course of the curves is practically the same for all investigated samples (see Fig. 3/a). This is an indication on the formation of stable Mo-O network structure, even if the sample contains boron oxide network former. The observed Mo-O distance is somewhat greater than the 1.75(5)Å distance reported for glassy $90MO_3$-$10Nd_2O_3$ from EXAFS measurements [23], and shows similarity to the Mo-O 1.73-1.82Å distances in crystalline $LaBMoO_6$ [24] and in Nd_2O_3-MoO_3 [5]. The Mg-O first neighbour distance is obtained also at 1.8±0.1Å, but its accuracy is considerably less than that of the Mo-O distance. This is partly because its relatively low concentration, especially for the Mo80Nd15Mg5 sample, and also due to the low scattering amplitude of Mg for both radiations, resulting in low weighting factors. For the Mo75Nd12.5Mg12.5 sample the Mg-O distributions show a second peak at 2.1±0.1Å, this can overlap with the Nd-O distances. The Nd-modifier shows characteristic Nd-O first neighbour distance at 2.05Å, and a next one at 2.85Å for the binary Mo90Nd10, while for the other compositions the first neighbour distance shifts to slightly higher distances 2.1-2.3Å. The intensity decreases and the peak is less characteristic inspite of the increased Nd-concentration in the ternary samples. The reason for this result may be in the more complicated network due to the increased number of constituent components. The small peak at 2.85Å seems to be reproducible, however, the peak position agrees with the second O-O distance, thus its origin may be artificial. The Nd-O distances reported in the literature are somewhat greater than our results, i.e. 2.51-2.73Å in glassy MoO_3-Nd_2O_3 [8], 2.33-2.5Å in crystalline Nd_2O_3-MoO_3 [5], 2.24-2.32 Å in $Y_{2-x}Nd_xMo_4O_{15}$ [25]. The O-O distribution shows two characteristic peaks at 2.4 and 2.8Å (see Table 2). We assume that the shorter distance belongs to the B-O network, while the longer distance to the Mo-O network. The B-O distribution function shows a relatively broad first neighbour distance at 1.40±0.05Å with a half-width value of 0.25Å, is usually the case for B-O network [18, 22].

Figure 4 shows the coordination number distributions as revealed from the RMC simulation, while the corresponding average coordination numbers, CN_{ij} are tabulated in Table 3.

In the high Mo-containing binary Mo90Nd10 sample the average number of oxygen atoms around Mo is 4.9±0.2 atoms. We have investigated the possibility of a mixed network, containing both MoO_4 and MoO_6 units, by RMC simulation. If we suppose that MoO_4 units similarly to the crystalline $LaBMoO_6$ [24], Nd_2O_3-MoO_3 [5] and usually this is the case for molybdate crystals. For glassy molybdate network the presence of MoO_4^{-2} units were reported [9, 10, 21], while the formation of MoO_6 units was also observed, they are present in the network. In case of binary system it would mean that 55% of the

Mo atoms are 4-fold oxygen coordinated, while 25% are 6-fold coordinated, while the rest 20% are in 3- and 5-fold coordinated states, with an error about 5%. Taking into consideration the $g_{Mo\text{-}O}(r)$ distribution, we can establish that the shorter distance at 1.8Å can be attributed to the MoO_4 units, while in addition two further oxygen neighbours appear at a longer 2.0Å distance forming MoO_6 units.

According to Table 3, with decrease of Mo content the number of oxygen neighbours slightly decreases to 4.0 atoms. For the Mo80Nd15Mg5 and Mo75Nd12.5Mg12.5 ternary samples the average coordination number, as calculated from the RMC modeling, is $CN_{Mo\text{-}O}$=4.2 and 4.0±0.2 atoms, respectively. As far as, the corresponding $g_{Mo\text{-}O}(r)$ distributions contains a characteristic peak at 1.8Å and small shoulder at 2.1Å, we may conclude that 87 and 98% of the Mo atoms form MoO_4 units, while about 8% and 0% form MoO_6 units in case of Mo80Nd15Mg5 and Mo75Nd12.5Mg12.5 samples, respectively. For the Mo50Nd25B25 sample the average coordination number is $CN_{Mo\text{-}O}$=4.2±0.2 atoms. The $g_{Mo\text{-}O}(r)$ distributions besides well known 1.8Å peak show a small "sub"-peak at 2.0Å, than we may conclude that 72% of the Mo atoms form MoO_4 units, while about 10% form MoO_6 units, the rest 18% are in 3- and 5-fold coordinated states, with an error about 5-7%. In case of ternary systems distortion of the tetrahedral MoO_4 units can not be excluded.

The average number of oxygen neighbours of the modifier Nd is 4.3 atoms for both the binary Mo90Nd10 and for the boron-containing ternary sample, while it is significantly smaller for the Mg containing samples, 3.1 atoms. The reason may be that Mg is also a modifier, which plays a similar role like Nd, increasing the number of non-bridging oxygen (NBO) atoms.

The Mg-O coordination number is 4.3 and 3.8 close to form tetrahedral units, for Mo80Nd15Mg5 and Mo75Nd12.5Mg12.5, respectively. The average coordination number suggests that Mg^{2+} cation can act as a conditional network-former. The Mg-O bond distances were in the range 1.8-2.1 Å, in accord with the values experimentally reported for Mg^{2+} cations in tetrahedral coordination [26].

The boron atoms are coordinated mostly by 3 and 4 oxygen atoms, forming trigonal BO_3 and tetrahedral BO_4 units, similarly to other boron containing networks containing modifier atoms as discussed above (see i.e. refs [9-10, 20-22]). The RMC model calculation results not only 3- and 4-fold oxygen coordinated boron atoms, but also 2 oxygen neighbours (Fig. 5/c). This may be an artificial consequence of RMC modelling, as far as the calculation starts from a random distribution of the atoms packed in the simulation box. The relative amount of the different coordinated boron is an important question, especially the number of BO_3 and BO_4 units. Nd_2O_3 acting as modifier causes partial conversion of BO_3 and BO_4 groups leading to the formation of NBO. For Mo50Nd25B25 sample ~68% of B-atoms are 3-coordinated, while ~30% are 4-coordinated, while the rest 2% are in 2-fold coordinated states, with an error about 3%, the average coordination number is 3.3 atoms.

The O-O average coordination number is 8 atoms for the 2-component Mo90Nd10 sample, which is the highest among the investigated samples. The average O-O coordination number reduces to 6 atoms for the samples with increasing number of contributing components, which may be the consequence of mixed structural units.

The RMC modelling also provides information on the second coordination sphere. The basic question is, whether the linkage of the basic structural units show any correlation or not? The analysis of the metal-metal and boron-metal pair correlation functions show pronounced correlations, the corresponding atomic pair distances are shown in Fig. 5. The shortest second neighbour distances are obtained for B-B as 2.7Å, Mo-B 2.9Å which indicate mixed linkages, and Mo-Mg 2.8Å which is related to NBO bond. These results indicate the existence of a pronounced intermediate-range ordering.

5. Conclusions

Rare-earth molybdate glasses have been prepared by melt quenching technique, and the network structure was investigated by neutron and high-energy X-ray diffraction. For data evaluation the RMC simulation technique was applied to obtain a possible 3-dimensional network configuration, which is consistent with the experimental data. The RMC simulation box did contain 10000 atoms and the

usual constraints were applied, i.e. atomic density, cut-off distances (nearest neighbour distances for all atom pairs) and connectivity. From the RMC modelling the partial atomic correlation functions $g_{ij}(r)$ and the coordination number distributions CN_{ij} have been revealed. Formations of MoO_4 units were estabilished with 1.80Å Mo-O distance. In the binary glass MoO_4 (55%) and MoO_6 (25%) structural units were revealed. In ternary systems mainly MoO_4 units are present, and with decreasing MoO_3 concentration, the ratio of MoO_6 units roughly decreases. For the B-containing ternary glasses B-O first neighbour distance was obtained at 1.40Å, the B-O network is formed by BO_3 and BO_4 groups. Mixed MoO_4-BO_4 and MoO_4-BO_3 linkages form pronounced intermediate-range order.

Acknowledgement
The authors are grateful to Drs. Gy. Mészáros, L. Alexandrov and Prof. Y. Dimitriev for their helpful contribution in this work. The authors would like to thank Drs. Anna Llobet and Martin von Zimmermann instrument scientists at the neutron- and X-ray diffraction experimental stations at the HIPD (Lujan Neutron Scattering Centre) and BW5 (Hasylab at Desy). The research was supported by the EU-FP7-NMI3 No.283883. Thanks to the financial support of Hungarian OTKA-PD 109384 and to the bilateral cooperation of Hungarian-Bulgarian Academy of Sciences SNK-63/2013.

References
[1] Lacorre P, Goutenoire F, Bohnke O, Retoux R, Laligant Y 2000 *Nature* **404** 856
[2] Georges S, Goutenoire F, Bohnke O, Steil M C , Skinner S J, Wiemhöfer H D, Lacorre P 2004 *J. New Mat. Electrochem. Systems* **7** 51
[3] Kato A, Uchitomi N, Oishi S, Shishido T, Iida S 2006 *Physica Status Solidi (c)* **3(8)** 2709
[4] Naruke H, Yamase T 2003 *Journal of Solid State Chemistry* **173** 407
[5] Barker R S, Evans I R 2006 *Journal of Solid State Chemistry* **179** 1918
[6] Zhao D, Cheng W D, Zhang H, Hang Fang S P 2008 *Dalton Transactions* **28** 3709
[7] Atuchin V V, Chimitova O D, Gavrilova T A, Molokeev M S, Kim S J, Surovtsev N V, Bazarov B G 2011 *Journal of Crystal Growth* **318** 683
[8] Alexandrov L, Iordanova R, Dimitriev Y, Hamda K, Ide J, Milanova M 2008 *Advanced Materials Research* **39-40** 37
[9] Aleksandrov L, Iordanova R, Dimitriev Y 2009 *Journal of Non-Crystalline Solids* **355** 2023
[10] Aleksandrov L, Komatsu T, Iordanova R, Dimitriev Y 2011 *Journal of Physics and Chemistry of Solids* **72** 263
[11] R McGreevy R L, Pusztai L 1988 *Mol. Simul.* **1** 359; http://www.szfki.hu/~nphys/rmc++/opening.html
[12] Sváb E, Mészáros Gy, Deák F 1996 *Materials Science Forum* **228** 247; http://www.bnc.hu/
[13] Proffen Th, Billinge S J L, Egami T, Louca D 2003 *Zeitschrift für Kristallographie* **218** 132
[14] Ambroise J P, Bellissent R 1984 *Rev. Phys. Appl.* **19** 731; http://www-llb.cea.fr/en/
[15] Poulsen H, Neuefeind J, Neumann H B, Schneider J R, Zeidler M D 1995 *J. Non-Cryst. Solids* **188** 63
[16] Hannon A C, ISIS Disordered Materials Database 2006, http://www.isis.rl.ac.uk/disordered
[17] Waasmaier D, Kirfel A 1995 *Acta Crystallogr. A* **51** 416
[18] Fábián M, Sváb E, Proffen Th, Veress E 2008 *Journal of Non-Crystalline Solids* **354** 3299
[19] Fabian M, Proffen Th, Ruett U, Veress E, Svab E 2010 *J. Phys.: Condens. Matter* **22** 404206
[20] Burns A E, Winslow D W, Clarida W J, Affatigato M, Feller S A, Brow R K 2006 *Journal of Non-Crystalline Solids* **352** 2364
[21] Iordanova R, Aleksandrov L, Bachvarova-Nedelcheva A, Ataala M, Dimitriev Y 2011 *Journal of Non-Crystalline Solids* **357** 2663
[22] Fábián M, Sváb E, Proffen Th, Veress E 2010 *Journal of Non-Crystalline Solids* **356** 441
[23] Alexandrov L, Iordanova R, Dimitriev Y 2007 *Phys. Chem. Glasses: European J. Glass Sci. Technol. B.* **48(4)** 242
[24] Wang Z, Zhang L, Wang G, Song M, Huang Y, Wang G 2009 *Optical Materials* **31** 849
[25] Wang H, Peng J, Chen D F, Hu Z 2006 *Solid State Sciences* **8** 1144
[26] Deng F, Yue Y, XiaoT, Du Y, Ye Ch, An L, Wang H 1995 *J. Phys. Chem.* **99** 6029